

# Alternate energy transduction routes in chemically skinned rabbit psoas muscle fibres: a further study of the effect of MgATP over a wide concentration range

ROBERT N. COX and MASATAKA KAWAI

*Muscle Physiology Division, Department of Neurology, Columbia University, 630 West 168th Street, New York, New York 10032, U.S.A.*

Received 8 October 1980

---

## Summary

Complex stiffness data were studied over an extended range of MgATP concentrations ( $3\ \mu\text{M}$ – $5\ \text{mM}$ ) in single fibres of  $\text{Ca}^{2+}$ -activated, chemically skinned adult rabbit psoas. The data were analysed in terms of a model involving three exponential processes, the presence of which was previously observed in fully activated muscles. As fibres were transferred from a rigor solution into solutions of gradually increasing MgATP concentration, the three processes appeared sequentially, each with a unique  $K_m$ . The order of appearance as MgATP increases is (1) the slowest of the three processes [designated process (A)], (2) the fastest of the three processes [designated (C)], and (3) process (B), which occupies the middle range of frequencies; the  $K_m$ s are approximately  $10\ \mu\text{M}$ ,  $0.2\ \text{mM}$ , and  $0.8\ \text{mM}$ , respectively. The single phase advance [process (A)] remaining at very low substrate concentrations was found to be better described by a distribution of rate constants than by a single rate constant. The influence of substrate concentration on these processes is examined and two parallel hydrolysis routes are suggested as a possible mechanism.

## Introduction

Since Huxley & Simmons (1971) identified four phases in the tension transient following a step-length change in activated intact skeletal muscles, much of our effort has been devoted to correlating these transients with underlying chemomechanical processes in skinned fibre preparations. These preparations allow the bathing medium of the contractile proteins to be controlled and the results to be readily compared with those of biochemical experiments. Our own studies have shown the transients to be absent in muscles that are relaxed or are in a rigor state, which

supports the interpretation that the transients reflect kinetics of actively cycling crossbridges (Kawai *et al.*, 1977; Kawai & Brandt, 1980).

We study these transients by changing the length of the muscle according to a sinusoidal waveform at varying frequencies and by observing the amplitude and phase shift of the tension response. In this way magnitude and rate-constant parameters equivalent to those deduced with the step-length change technique could be derived. The sinusoidal technique is employed because the signal-to-noise ratio is superior and the temporal resolving power is greater than those given by other techniques, although a longer time is required for a measurement.

In our investigations, three exponential processes are identified in muscles exposed to saturating concentrations of MgATP and  $\text{Ca}^{2+}$ . These processes were designated (A), (B), (C), corresponding to phases 4, 3, 2, respectively, of Huxley (1974) (for correlations, see Kawai & Brandt, 1980). (Phase 1, corresponding to the instantaneous stiffness  $Y_{\infty}$  and presumably arising from the elasticity of the muscle, is qualitatively different from the other three phases or processes.) In our previous studies it was demonstrated that changing the concentration of MgATP (substrate for actomyosin ATPase) in the low mM range affects the rate constants of processes (B) and (C) (Kawai, 1978, 1979), whereas varying the concentration of  $\text{Ca}^{2+}$  affects primarily process (B) (Kawai *et al.*, 1981). These observations are taken as evidence that process (B) reflects the state of actin, whereas the detachment transition dominates process (C) in vertebrate skeletal muscle subjected to physiological concentrations of MgATP and Ca.

In the present study substrate concentrations were extended to the  $\mu\text{M}$  range (keeping  $\text{Ca}^{2+}$  at saturating levels) and the exponential processes were examined starting from rigor. A strikingly different kinetic picture was found in the very low substrate range: only a single process (A) is present, and its centre in the Nyquist plot is displaced below the abscissa, implying distributed rate constants such as described by Cole & Cole (1941). In addition, each of the exponential processes was found to change, both in rate and magnitude, as the MgATP concentration was elevated from a few  $\mu\text{M}$  to mM levels.

## Materials and methods

All experiments were performed on chemically skinned single fibres of adult rabbit psoas. Both fresh preparations (<10 days old, maintained in relaxing solution at  $2^{\circ}\text{C}$ ) and stored preparations (<4 months old, maintained in isoionic relaxing saline with 6 M glycerol at  $-20^{\circ}\text{C}$ ) were used in the present study, with no significant difference in result. Details of the chemical skinning and storage procedures have been described elsewhere (Eastwood *et al.*, 1979). A segment of a single fibre 5–8 mm long was dissected from a stock bundle and transferred to an experimental chamber machined from a solid block of aluminum. The ends of the muscle fibre segment were wrapped around and clipped into two stainless steel tubes (see Brandt *et al.*, 1980, for method of mounting), one of which is connected to a length driver and the other to an Aker's AE801 force transducer assembly (Aker's Micro-Electronics, Horten, Norway; Brandt *et al.*, 1976). Muscle length was adjusted to approximately 10% above slack length ( $L_0$ ), which generally yields sarcomere lengths in the range 2.5–2.6  $\mu\text{m}$ .

In our experiments the length of the muscle is oscillated sinusoidally at 17 frequencies between 0.125 and 167 Hz. The sine waves are synthesized by a Nova 4S computer (Data General Corp.) and applied to the length control device. The peak-to-peak length oscillation is restricted to 0.2%  $L_0$  ( $\pm 1.3$  nm per half sarcomere), and the concomitant amplitude and phase shift (complex stiffness) in tension are observed and graphed as frequency plots (Fig. 2) or as Nyquist plots (Fig. 3). The complex stiffness data  $Y(f)$  are standardized to the size of the fibre, yielding 'complex modulus':  $Y_M(f) = Y(f) (L_0/A_0)$ , where  $A_0$  is the cross-sectional area. Experimental and analytical details have been described (Kawai & Brandt, 1980).

The protocol for mixing solutions is as follows. First, the  $\text{MgATP}^{2-}$  (variable),  $\text{CaATP}^{2-}$  (2.38 mM), and  $\text{ATP}^{4-}$  (1 mM) concentrations are specified. Then the concentrations of  $\text{Ca}^{2+}$  and  $\text{Mg}^{2+}$  are calculated based on the mass action law:

$$\begin{aligned} [\text{CaATP}^{2-}] &= K_{\text{CaATP}}[\text{Ca}^{2+}][\text{ATP}^{4-}] \\ [\text{MgATP}^{2-}] &= K_{\text{MgATP}}[\text{Mg}^{2+}][\text{ATP}^{4-}] \end{aligned}$$

where apparent association constants (at pH 7.00) used are:  $K_{\text{CaATP}} = 5 \text{ mM}^{-1}$ ,  $K_{\text{MgATP}} = 10 \text{ mM}^{-1}$ . The total concentrations of  $\text{Ca}^{2+}$ ,  $\text{Mg}^{2+}$ , and ATP to be added are given by:

$$\begin{aligned} [\text{Ca}]_{\text{total}} &= [\text{Ca}^{2+}] + [\text{CaATP}^{2-}] = 2.86 \text{ mM} \\ [\text{Mg}]_{\text{total}} &= [\text{Mg}^{2+}] + [\text{MgATP}^{2-}] \\ [\text{ATP}]_{\text{total}} &= [\text{CaATP}^{2-}] + [\text{MgATP}^{2-}] + [\text{ATP}^{4-}]. \end{aligned}$$

Calcium is added in the form of calcium propionate, magnesium in the form of  $\text{Na}_2\text{MgATP}$  (premixed at 1:1), and remaining ATP in the form of  $\text{Na}_4\text{ATP}$ . For calculating ionic strength, monovalent (sodium, propionate, 1/2 of imidazole) and divalent (sulphate, creatine phosphate, EGTA) ions are assumed to exist exclusively in dissociated forms. It is also assumed that  $\text{CaATP}$  and  $\text{MgATP}$  are divalent anions, that free ATP is 76% tetravalent and 24% trivalent, that phosphate is 63% monovalent and 37% divalent, and that EDTA is 87% trivalent and 13% divalent at pH 7.00 (after  $\text{H}^+$  association constants extracted from Martell, 1964). The result of these calculations is listed in Table 1. The activating solutions also contained (sodium salts): 7.5 mM phosphate, 15 mM creatine phosphate (CP), and 74 unit/ml creatine phosphokinase (CPK). Ionic strength was adjusted to 200 mM with Na propionate and  $\text{Na}_2\text{SO}_4$ . In order to maintain both ionic strength and monovalent cation ( $\text{Na}^+$ ) concentration constant, increase in substrate ( $\text{Na}_2\text{MgATP}$ ) concentration was compensated by an identical decrease in the concentration of  $\text{Na}_2\text{SO}_4$ .  $p\text{Ca}$  refers to  $-\log[\text{Ca}^{2+}]$ . All solutions were buffered with 6 mM imidazole to pH  $7.00 \pm 0.01$ , temperature was controlled to  $20.0 \pm 0.1^\circ \text{C}$ , and the saline bathing the fibre was constantly stirred.

## Results

Before beginning the varying  $\text{MgATP}$  series, all fibres were activated with a solution containing 5 mM  $\text{MgATP}$  and 0.476 mM  $\text{Ca}^{2+}$  to collect control isometric tension ( $P_0$ ) and complex stiffness data. The  $P_0$  averaged  $1.2 \pm 0.4 \times 10^5 \text{ Nm}^{-2}$  ( $n = 12$ ;  $\pm$  indicates 1 S.D.). Typical complex stiffness data with three characteristic exponential processes were obtained. Following this activation, fibres were brought into the 'high-rigor state' (Kawai & Brandt, 1976) by washing with  $\text{Rg}_2$  solution (Table 1) and then returned to R. After several minutes in R, a 'low-rigor state' was induced by washing the fibres with  $\text{Rg}_1$  solution, which contains 10 mM EDTA. In single fibres of rabbit psoas a full low-rigor develops in less than 20 s as judged by the stiffness

**Table 1.** Composition of solutions used. The left-hand section of the table describes the actual procedure (species and concentrations mixed) that was followed to create each solution. The final concentrations of critical species, where different from the concentrations mixed together, are listed in the right-hand section of the table. Also, the pCa of Rg<sub>2</sub>, Rg<sub>3</sub> and all activating solutions is 3.3. The last digits of the MgATP concentrations represent the level of magnesium contamination and are therefore not significant.

Solution labels	Total added concentrations (mM)											Final concentrations (mM)				
	EGTA	EDTA	MgATP	ATP	CaProp <sub>2</sub>	Phosphate	Na <sub>2</sub> SO <sub>4</sub>	NaProp	CP	Imidazole	MgATP	CaATP	Mg <sup>2+</sup>	Free ATP		
R (relax)	5	—	2	—	—	8	39	43	—	6	—	—	—	—		
W (wash)	—	—	2	—	—	8	44	43	—	6	—	—	—	—		
Rg <sub>1</sub> (rigor)	—	10	—	—	—	8	27	43	—	6	—	—	—	—		
Rg <sub>2</sub> (rigor)	—	—	—	—	0.47	8	46	43	—	6	—	—	—	—		
Rg <sub>3</sub> (rigor)	—	—	—	—	0.47	8	31	43	15	6	—	—	—	—		
Activating solutions	—	—	0.003	3.38	2.86	7.5	26.3	36.6	15	6	0.003	2.38	0.0003	1		
	—	—	0.011	3.38	2.86	7.5	26.3	36.6	15	6	0.010	2.38	0.001	1		
	—	—	0.035	3.38	2.86	7.5	26.3	36.6	15	6	0.032	2.38	0.003	1		
	—	—	0.110	3.37	2.86	7.5	26.2	36.6	15	6	0.100	2.38	0.010	1		
	—	—	0.348	3.35	2.86	7.5	26.0	36.6	15	6	0.316	2.38	0.032	1		
	—	—	1.100	3.28	2.86	7.5	25.2	36.6	15	6	1.000	2.38	0.100	1		
	—	—	5.500	2.88	2.86	7.5	20.8	36.6	15	6	5.000	2.38	0.500	1		

time course. Two washes are found to be sufficient under our experimental conditions. This rigor is characterized by a moderate elastic modulus ( $3.5 \pm 2.3 \times 10^6 \text{ Nm}^{-2}$ ; measured at 100 Hz,  $n = 16$ ) and very low tension (average 2.6%  $P_0$ ; range 0–6%). The tension record and experimental protocol from a typical experiment are portrayed in Fig. 1. The frequency dependence of complex modulus data from low-rigor muscle is identical to that from a high-rigor muscle (Figs. 2, 3h) except for a scaling factor (low:high is  $0.38 \pm 0.12$ ,  $n = 7$ , measured at 100 Hz). The stiffness of the low-rigor muscle is small, presumably because crossbridges or in-series elements are slack in this condition, rather than because fewer bridges are attached (Kawai & Brandt, 1976). Complex modulus data from crayfish (Kawai *et al.*, 1977) and rabbit (Kawai & Brandt, 1980) fibres in high rigor were previously published.

After a few minutes the EDTA solution was replaced with a saline containing 0.47 mM  $\text{Ca}^{2+}$  (solution Rg<sub>2</sub> in Fig. 1), which produced little change in tension or modulus (stiffness ratio after:before was  $1.04 \pm 0.07$  at 100 Hz,  $n = 15$ ). This indicates that no large-scale attachment of crossbridges takes place as calcium is bound to troponin C in rigor; hence we can assume that virtually all of the crossbridges capable of attachment combine with actin when the low-rigor state develops (cf. Bremel & Weber, 1972; Kawai & Brandt, 1976). The fibre in rigor (with or without calcium) does not shorten when the ends are released (unpublished observations).

The solution was then replaced with one containing 15 mM CP and 74 unit/ml CPK in the presence of calcium (solution Rg<sub>3</sub> in Fig. 1). Thereafter the fibre was tested with increasing concentrations of MgATP, keeping calcium at saturating

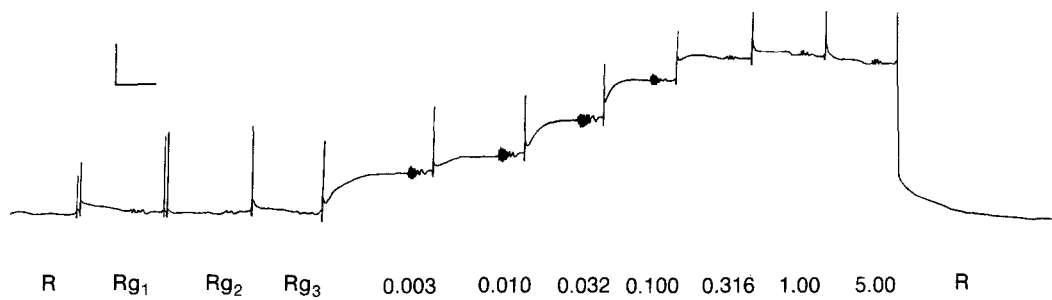


**Fig. 1.** Tension time course (traced from the original record) and experimental protocol. Calibrations are  $100 \mu\text{N}$  and 60 s. The sharp vertical lines are solution change artifacts. The horizontal bars represent time spans during which complex stiffness data were collected. Oscillation in the tension trace is visible in some of the records. The higher frequency oscillations are not visible because the tension signal was filtered at 10 Hz (low pass Butterworth) before tracing. Also indicated are the solutions (numbers are MgATP concentrations, mM; Table 1) in which the fibre was bathed for each record. The slow relaxations of tension following solution changes Rg<sub>1</sub>, Rg<sub>3</sub>, and R are due to temperature transients caused by adding slightly cold solutions.

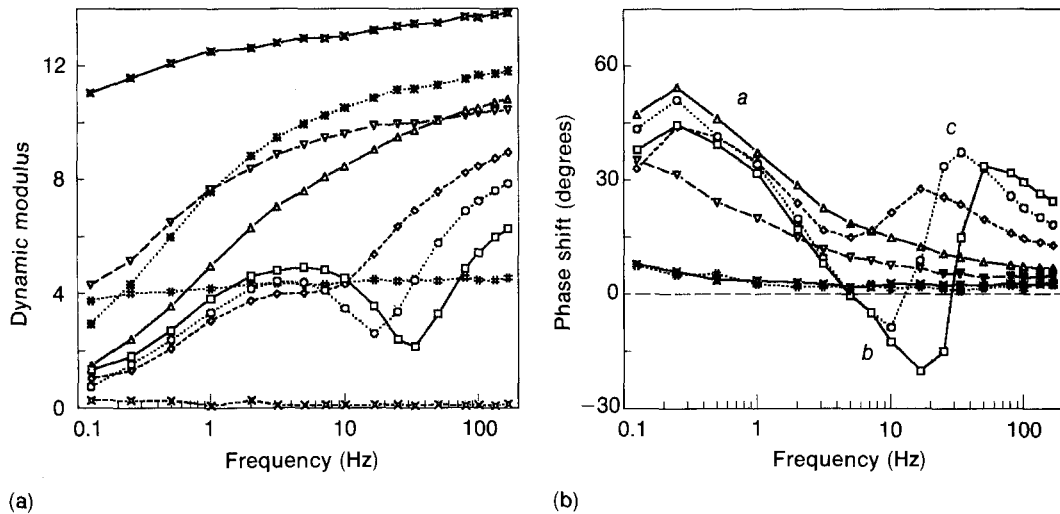


**Fig. 2.** Plots of complex modulus  $Y_M(f)$  versus frequency from relaxed ( $\circ$ --- $\circ$ ), low-rigor ( $\#$ --- $\#$ , in  $Rg_3$  solution), and high-rigor ( $\nabla$ --- $\nabla$ , in  $Rg_2$ ) conditions, and at various substrate concentrations. Data were averaged from three experiments (average  $P_0$  was  $0.91 \times 10^5 \text{ N m}^{-2}$ ), except for the two rigor conditions which were taken from two independent experiments. In (a), dynamic modulus [ $|Y_M(f)|$ ] is plotted (units:  $10^6 \text{ N m}^{-2}$ ). In (b), phase shift [ $\arg(Y_M(f))$ ] is plotted, and the approximate locations of characteristic frequencies  $a$ ,  $b$ ,  $c$  are indicated. Data from the two rigor conditions are almost superimposed. The MgATP concentrations are 0.003 mM ( $\nabla$ --- $\nabla$ ), 0.03 mM ( $*$ --- $*$ ), 0.1 mM ( $\triangle$ --- $\triangle$ ), 0.3 mM ( $\diamond$ --- $\diamond$ ), 1 mM ( $\circ$ --- $\circ$ ), 5 mM ( $\square$ --- $\square$ ). Some of the curves from the original series are deleted to avoid crowding of data. All data are from experiments on single fibres.

concentrations. The first solution contained a total of 3.38 mM ATP (2.38 mM CaATP and 1 mM free ATP), without added magnesium. Contaminating magnesium, which comes mostly from ATP (purchased from Sigma Chemical Co.) and which we estimate to be 2–4  $\mu\text{M}$  (Reuben *et al.*, 1971), produces sufficient trace MgATP for the fibre to develop tension, although several minutes are required before a tension plateau is reached. After one set of complex modulus data were recorded, the MgATP concentration was sequentially incremented, and the modulus measurements were repeated. The time to reach plateau tension decreased at the higher substrate concentrations. In the experiment portrayed in Fig. 1, and in all other experiments, peak tension occurred at a MgATP concentration of 1 mM. The final solution in the series was the same as for the initial control activation (5 mM MgATP).  $P_0$  reproduced within  $88 \pm 8\%$  ( $n = 12$ ); the fibre was then returned to R. The fibre shortened at all substrate concentrations (3  $\mu\text{M}$ –5 mM) when the ends were released, and it redeveloped tension when held isometric after shortening.

Figs. 2 and 3 show a series of averaged complex modulus data obtained from similar experiments. The Nyquist plot from fibres exposed to saturating substrate concentrations (Fig. 3g) shows the characteristic three-arc structure, indicating the

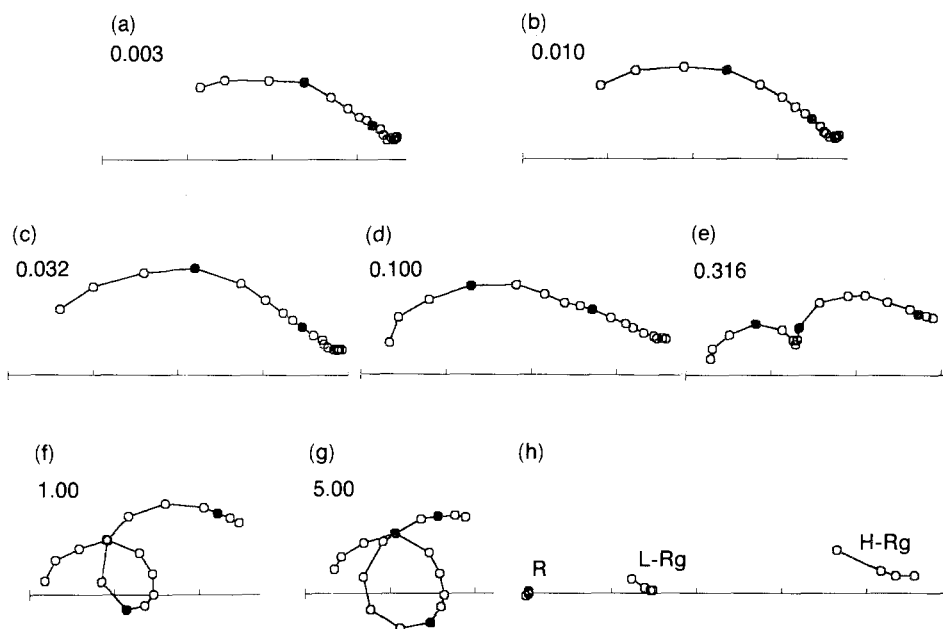


**Fig. 3.** The same data as in Fig. 2 are shown in Nyquist plots [*real* (abscissa) versus *imaginary* (ordinate) parts of the complex modulus data  $Y_M(f)$ ]. The origin is indicated by (o) to the left of each panel; each interval represents  $3 \times 10^6 \text{ N m}^{-2}$ . (a–g) Frequency values are (from left to right, each panel): 0.125, 0.25, 0.5, 1, 2, 3.13, 5, 7.14, 10, 16.7, 25, 33.3, 50, 80, 100, 133, 167 Hz (frequencies 1, 10 and 100 are indicated, where practical, by filled symbols). (h) 0.125, 1, 10, 100 Hz. Data from relaxed (R), low-rigor (L-Rg) and high-rigor (H-Rg) conditions are plotted. A 0.5 s delay follows the beginning of oscillation at each frequency so that steady-state sinusoidal tension oscillation is achieved before the beginning of data collection.

presence of at least three exponential processes in the length–tension reponse. We have named these processes (A), (B), (C) in the order of slow to fast (Kawai *et al.*, 1977). The corresponding transfer function is:

$$Y_M(f) = H + \frac{(A)}{1 + a/fi} - \frac{(B)}{1 + b/fi} + \frac{(C)}{1 + c/fi} \quad (1)$$

where  $A, B, C$  are magnitudes;  $a, b, c$  are the characteristic frequencies ( $a < b < c$ );  $f$  is frequency, and  $H$  is a constant. Process (A) is a low-frequency exponential lead, (B) a middle-frequency delay, and (C) a high-frequency lead. In the region of process (B), centering around 17 Hz, the muscle generates ‘oscillatory work’ (Pringle, 1967).

When substrate concentration is lowered, the modulus plots change drastically. Between 0.3 and 1 mM, both the magnitude and characteristic frequency of process (B) decrease markedly. [See lessening and disappearance of dip in Fig. 2a, and shift of the minimum to left in Fig. 2b; see the shape of (B) loop in Fig. 3e–g.] At

0.3 mM, only processes (A) and (C) are identifiable (Fig. 3e). It may be that magnitude  $B$  is too small to be resolved at this substrate concentration. Its disappearance is reminiscent of the 'high-tension state' observed in insect muscles (Pringle, 1967). Process (C) in the meantime shrinks (smaller  $C$ ) and slows down (smaller  $c$ ), disappearing at MgATP concentrations of 32  $\mu\text{M}$  or less (Fig. 3c). Only a hint of (C) remains in Fig. 3d.

The high-frequency stiffness is greatest at 32  $\mu\text{M}$  MgATP (Fig. 2a), where it is 82% ( $\pm 11\%$ ,  $n = 6$ ) of the average high-rigor stiffness. Both steady-state tension and high-frequency stiffness data are comparable to earlier data obtained from crayfish muscle preparations (Kawai & Brandt, 1977).

Finally, over the MgATP concentration range 3–32  $\mu\text{M}$ , only the lower frequency lead [process (A)] is apparent. Examination of Fig. 3a–c shows that at very low substrate concentrations the complex modulus locus is a circular arc the centre of which is displaced below the abscissa. An empirical transfer function describing such a phenomenon is:

$$Y_M(f) = H + A/[1 + (a/ff^k)] \quad (2)$$

where  $0 < k \leq 1$  (adapted from Cole & Cole, 1941). One implication of such a function is that the characteristic frequency (hence the rate constant) is distributed around a centre value (Bottcher, 1952; see also Chaplain & Frommelt, 1968; Abbott, 1973), rather than being single-valued.  $k = 1$  for no distribution, and  $k$  is progressively smaller for wider distribution. The centre of the circular arc becomes increasingly displaced below the abscissa as  $k$  becomes smaller.

We fit the complex modulus data to equation 2 by assuming  $H = 0$ , which is a good approximation at high substrate concentrations. The fitting was performed by eye after matching the arc with circles of varying radii. It was found that the characteristic frequency  $a$  decreases over the MgATP concentration range 1 mM–3  $\mu\text{M}$  (from 1 to 0.4 Hz), with a  $K_m$  [that is, that MgATP concentration at which the rate constant of process (A) assumes half its maximal value] of the order of 10  $\mu\text{M}$ . This value varied by  $\pm 50\%$  due to uncertainty in magnesium contamination and difficulty in fitting data to equation 2. Also,  $k$  gradually decreases from 0.95 (1 mM MgATP) to 0.65 (3  $\mu\text{M}$  MgATP). Magnitude  $A$  is approximately constant over the MgATP concentration range 3–30  $\mu\text{M}$  and is over three-fold greater at this substrate range than at 5 mM MgATP. The  $K_{ms}$  for processes (B) and (C), estimated by fitting the rate-constant data to a Michaelis–Menten type of hyperbolic equation (Kawai, 1979), were found to be 0.8 mM and 0.2 mM, respectively. These values vary by  $\pm 20\%$  depending on the measurement.

The observations described above are not the result of an insufficient concentration of ATP or of an accumulation of ADP in the core of the fibre. Previous experiments (Kawai & Brandt, 1979) in which we have varied the CP (0–20 mM), CPK (0–80 unit  $\text{ml}^{-1}$ ), and free ATP (1–10 mM) concentrations in the presence/absence of stirring under conditions in which the apparent rate constants of actomyosin interaction



depend heavily on the ATP backup system (pCa 3.3, 0.25–10 mM MgATP) demonstrate that MgATP is more than adequately buffered under the conditions of the present study, that is, 15 mM CP, 74 U ml<sup>-1</sup> of CPK, and 1 mM free ATP.

## Discussion

The major finding of the present study is that the three exponential processes appear sequentially and saturate (each with a unique  $K_m$ ) as the MgATP (substrate) concentration is elevated (Figs. 2, 3). The first process to appear is (A), which becomes evident when a few  $\mu\text{M}$  of substrate are added to the rigor muscle ( $K_m = 10 \mu\text{M}$ ). The second is process (C), which appears at sub-mM concentrations of substrate ( $K_m = 0.2 \text{ mM}$ ). The third and last process to emerge is (B), which appears and saturates in the range of mM concentrations of MgATP ( $K_m = 0.8 \text{ mM}$ ). Hence we have the interesting result that the binding and hydrolysis of MgATP can limit the rate of each of the three processes depending on substrate concentration.

At very low MgATP concentrations the myosin heads are presumably attached to actin in rigor-like bonds, and therefore substrate binding and/or head dissociation must be rate-limiting for process (A). Because we can assume that the strain on the crossbridges is distributed, the intrinsic rate constants which contribute to process (A) must also be distributed. This follows from the widely held belief that the detachment rate is strain sensitive (Huxley, 1957; White & Thorson, 1972; Podolsky & Nolan, 1973; Julian *et al.*, 1974) and is supported by direct measurements of our own (Kawai & Brandt, 1976). At higher substrate concentrations the myosin heads spend less time in the rigor configuration, and therefore the distributed nature of crossbridge strain becomes less obvious. This explains why  $k$  in equation 2 is smaller at lower substrate concentrations and approaches unity when the substrate concentration is elevated.

Another important observation is that the muscle contracts (shortens) when the ends are released over the entire MgATP concentration range studied. Also, tension redevelops when the muscle is held isometric following a length release. This means that the muscle is capable of performing unidirectional work, even in MgATP concentrations too low to detect oscillatory work. When the substrate concentration is elevated to the mM range, the muscle becomes capable of performing oscillatory work also, as shown by the appearance of process (B) at frequencies around 7–25 Hz (Figs. 2b, 3f,g). Oscillatory work implies the ability to produce net work against an oscillating length driver in this specific frequency range. Both unidirectional work and oscillatory work use MgATP as the energy source.

It has been generally accepted that substrate binds to rigor-like actomyosin linkages and dissociates nucleotide-bound myosin from actin (Lymn & Taylor, 1971). After hydrolysis-product formation, the myosin reattaches to actin when the thin filament is turned on by Ca<sup>2+</sup> binding. This cyclic interaction between actin and myosin is consistent with unidirectional work [hence processes (A) and (C)], because

detachment and reattachment are prerequisites for gross muscle shortening. The effect of physiological substrate concentrations on process (C) can be understood in terms of the binding of MgATP to rigor-like linkages and the subsequent rapid dissociation of actin from myosin, as we reported earlier (Kawai, 1978, 1979).

It is not clear to us that the results of the present study can be modelled in terms of a simple cyclical scheme for actomyosin interaction with only one transition affected by MgATP. Of course, the number of apparent rate constants in such a scheme can in principle vary (depending on the relative values of the intrinsic rate constants) as the concentration of a species such as MgATP varies, but our attempts to understand quantitatively the results reported here in terms of such a model have been unsuccessful. While we cannot as yet rule out a model of this type, a scheme involving two (or perhaps more) parallel pathways for ATP hydrolysis seems more likely to lead to useful insights.

One example of such a scheme is suggested by the work of Tonomura (1978), Stein *et al.* (1979) and Eisenberg & Greene (1980), who have proposed that substrate binding, hydrolysis, and the transduction process can all take place without detachment of myosin from actin. While there remains a pathway common to the classical Lynn & Taylor (1971) scheme for the steps from energy transduction to substrate binding, product formation can take place via a parallel pathway that does not involve complete actomyosin dissociation. We are tempted to speculate that this alternate route is the basis of oscillatory work, although such speculation may be contradicted by Steiger *et al.*'s (1978) observation that stiffness increases with length in cardiac muscles. In order to produce oscillatory work, the myosin heads need perform only low amplitude cyclic motion, which could be achieved without complete dissociation of the head from actin. Whether a mechanism of this type or one involving ordinary attachment/detachment transitions is the molecular basis of oscillatory work, the results of the present study clearly establish that significantly different molecular events must underlie MgATP hydrolysis and energy transduction in widely disparate MgATP concentrations.

### Acknowledgement

We thank Drs M. Orentlicher and P. W. Brandt for helpful comments and criticism during the preparation of this manuscript. This work was supported in part by grants from NSF (PCM78-08592, PCM80-14527) and NIH (AM21530, NS05910).

### References

- ABBOTT, R. H. (1973) The effects of fibre length and calcium ion concentration on the dynamic response of glycerol extracted insect fibrillar muscle. *J. Physiol., Lond.* **231**, 195-208.
- BÖTTCHER, C. J. P. (1952) *Theory of Electrical Polarization*, pp. 363-374. Amsterdam: Elsevier.
- BRANDT, P. W., CHAPPELL, E. & JEWELL, B. R. (1976) A robust transducer suitable for measuring forces of 1  $\mu$ N. *J. Physiol., Lond.* **258**, 43-4P (abstract).

- BRANDT, P. W., COX, R. N. & KAWAI, M. (1980) Can the binding of  $\text{Ca}^{2+}$  to two regulatory sites on troponin-C determine the steep pCa/tension relation of skeletal muscle? *Proc. natn. Acad. Sci. U.S.A.* **77**, 4717–20.
- BREMEL, R. D. & WEBER, A. (1972) Cooperation within actin filament in vertebrate skeletal muscle. *Nature New Biol.* **238**, 97–101.
- CHAPLAIN, R. A. & FROMMELT, B. (1968) On the contractile mechanism of insect fibrillar flight muscle. I. The dynamics and energetics of the linearized system. *Kybernetick* **5**, 1–17.
- COLE, K. S. & COLE, R. H. (1941) Dispersion and absorption in dielectrics. I. Alternating current characteristics. *J. Chem. Phys.* **9**, 341–51.
- EASTWOOD, A. B., WOOD, D. S., BOCK, K. L. & SORENSON, M. M. (1979) Chemically skinned mammalian skeletal muscle. I. The structure of skinned rabbit psoas. *Tiss. Cell* **11**, 553–66.
- EISENBERG, E. & GREENE, L. E. (1980) The relation of muscle biochemistry to muscle physiology. *Ann. Rev. Physiol.* **42**, 293–309.
- HUXLEY, A. F. (1957) Muscle structure and theories of contraction. *Prog. Biophys.* **7**, 255–318.
- HUXLEY, A. F. (1974) Muscular contraction. *J. Physiol., Lond.* **243**, 1–43.
- HUXLEY, A. F. & SIMMONS, R. M. (1971) Proposed mechanism of force generation in striated muscle. *Nature, Lond.* **233**, 533–8.
- JULIAN, F. J., SOLLINS, K. R. & SOLLINS, M. R. (1974) A model for the transient and steady-state mechanical behavior of contracting muscle. *Biophys. J.* **14**, 546–62.
- KAWAI, M. (1978) Head rotation or dissociation? A study of exponential rate processes in chemically skinned rabbit muscle fibers when MgATP concentration is changed. *Biophys. J.* **22**, 97–103.
- KAWAI, M. (1979) Effect of MgATP on cross-bridge kinetics in chemically skinned rabbit psoas fibers as measured by sinusoidal analysis technique. In *Cross-bridge Mechanism in Muscle Contraction* (edited by SUGI, H. and POLLACK, G. H.), pp. 149–169. Tokyo: University of Tokyo Press.
- KAWAI, M. & BRANDT, P. W. (1976) Two rigor states in skinned crayfish single muscle fibers. *J. gen. Physiol.* **68**, 267–80.
- KAWAI, M. & BRANDT, P. W. (1977) Effect of MgATP on stiffness measured at two frequencies in  $\text{Ca}^{2+}$ -activated fibres. *Proc. natn. Acad. Sci., U.S.A.* **74**, 4073–5.
- KAWAI, M. & BRANDT, P. W. (1979) Effect of ATP buffer concentration on the mechanical rate constants in chemically skinned rabbit psoas fibers. *Biophys. J.* **25**, 270a (abstract).
- KAWAI, M. & BRANDT, P. W. (1980) Sinusoidal analysis; a high resolution method for correlating biochemical reactions with physiological processes in activated skeletal muscles of rabbit, frog and crayfish. *J. Mus. Res. Cell Motil.* **1**, 279–303.
- KAWAI, M., BRANDT, P. W. & ORENTLICHER, M. (1977) Dependence of energy transduction in intact skeletal muscles on the time in tension. *Biophys. J.* **18**, 161–72.
- KAWAI, M., COX, R. N. & BRANDT, P. W. (1981) Effect of Ca ion concentration on crossbridge kinetics in rabbit psoas fibres: Evidence for the presence of two Ca-activated states of thin filament. *Biophys. J.* (in press).
- LYMN, R. W. & TAYLOR, E. W. (1971) The mechanism of adenosine triphosphate hydrolysis by actomyosin. *Biochemistry* **10**, 4617–24.
- MARTELL, A. E. (1964) *Stability Constants of Metal-ion Complexes*. London: The Chemical Society.
- PODOLSKY, R. J. & NOLAN, A. C. (1973) Muscle contraction transients, cross-bridge kinetics, and the Fenn effect. *Cold Spring Harb. Symp. quant. Biol.* **37**, 661–8.
- PRINGLE, J. W. S. (1967) The contractile mechanism of insect fibrillar muscle. *Prog. biophys. molec. Biol.* **17**, 1–60.

- REUBEN, J. P., BRANDT, P. W., BERMAN, M. & GRUNDFEST, H. (1971) Regulation of tension in the skinned crayfish muscle fiber. I. Contraction and relaxation in the absence of Ca (pCa > 9). *J. gen. Physiol.* **57**, 385–407.
- STEIGER, G. J., BRADY, A. J. & TAN, S. T. (1978) Intrinsic regulatory properties of contractility in the myocardium. *Circulation Res.* **42**, 339–50.
- STEIN, L. A., SCHWARZ, R. P., CHOCK, P. B. & EISENBERG, E. (1979) Mechanism of actomyosin adenosine triphosphatase. Evidence that adenosine 5'-triphosphate hydrolysis can occur without dissociation of the actomyosin complex. *Biochemistry* **18**, 3895–909.
- TONOMURA, Y. (1978) Functional implications of the two-headed structure of myosin. *Sixth Int. Biophys. Cong. Abst.* 74.
- WHITE, D. C. S. & THORSON, J. (1972) Phosphate starvation and the nonlinear dynamics of insect fibrillar flight muscle. *J. gen. Physiol.* **60**, 307–36.